

# After buckling behavior of thin membranes and textiles based on tension field theory and experiments

Aura Conci

*UFF - Federal Fluminense University, RJ - Brazil*

## Abstract

This paper presents a study on the use of the tension field theory for efficient representation of fabrics. A highly buckled membrane model provides the simplest approach for visualization of vertical fabrics. The differential equation of tension lines gives the outline of the wrinkles. An equation system is presented, which, when iteratively solved supplies the basic variables of realistic fabric displacements: the number and positions of wrinkles, and the wrinkle depth. The model can also represent important physical characteristics of textiles, as malleability, elasticity and weight. Experimental measures have been developed as a way to verify the adequacy of the equations and to subsidize empirical propositions for improvement of the model. How to use this approach for textile visualization is the objective of this work. Although the original theory is complex, the resulting algorithm is simpler and faster than many numerical treatments already used for prediction of the cloth aspect. The idea is to find a simple realistic model that turns possible the addition in the displacement field of other important necessities of the fashion industry like animations and textures.

Keywords: tension field, theory of membranes, wrinkle lines, fabric displacements, post-buckling behavior, deformation of textiles.

## 1 Introduction

Realistic visualization of fabric has been the subject of many works because it is essential in computer-aided apparel design and fashion industry [1]. The main difficulty in realistic simulation of cloth is that its surface tends to look artificial in usual representation [2]. For modeling the way in which a cloth hangs, folds and wrinkles must be represented, as well as cloth's physical properties such as rigidity, elasticity and yarn structure. These characteristics distinguish a fabric from other materials. Moreover, they are associated with the aesthetic aspect of the garments.

The task of realistic visualization of cloth is much more difficult than a representation of its surface texture and has been considered usually by complex approaches [3]. Attempts to use finite element analysis and high-level mathematical techniques to model textiles demand vast computer power and yet still do not produce faithfully simulations of fabrics [4]. An experimental evaluation must be con-

28 sidered to maintain the aesthetic aspect. When fabrics are modeled as a physical object, even a single  
29 piece draping on an object (like table linings and curtains) may need a great amount of calculations  
30 [5]. The scale of the problem increases when fabric properties (elasticity, weight, etc.) must be taken  
31 into account and increase more when the problem moves from modeling only the appearance to exper-  
32 imental comparison of results. Computer model of fabrics has achieved a certain success (in computer  
33 graphics) but it has yet space to combine reality with mathematical models for an efficient graphi-  
34 cal representation. This work analyzes the use of the tension field theory combined with experimental  
35 measurements for fabric representation. This combination makes possible to characterize textile details  
36 in macro scale without the huge amount of computation necessary to micro scale representation, as  
37 that of approaches based on fibers or threads.

## 38 2 Basic considerations

39 Observing the fabrics we see that the textile structure can be considered as a membrane. Fabric  
40 folds are produced by gravity when only part of the cloth is directly supported. The lines of strain  
41 presented on buckled membrane or highly thin plate are referred to as wrinkle lines [6], and they  
42 represent the folds and the crinkles in fabrics [7]. The relationship between the membrane surface and  
43 the load direction is very important in the mechanical behavior. There is no external loading in many  
44 applications of textiles and the weight acts everywhere in vertical direction (due to the Earth gravity).  
45 Fabrics undergo large displacements for small applied forces. Their displacement properties depend  
46 on the textile surface direction. We shall distinguish between two essential kinds of behavior on these  
47 structures:

48 (1) Normal load - a textile with loads applied in direction normal or perpendicular to its initial  
49 plane (typical examples of this first type of behavior are a carpet falling on the floor, a waving flag,  
50 or a cloth being lifted from a flat surface); and

51 (2) In plane load - a textile which carry loads in the same directions of its plane (typical examples  
52 of this second type of behavior are vertical suspended blankets, curtains or a dress on a mannequin  
53 and other fashion applications,).

54 The effect of gravity is generally the main load on a fabric. Therefore in great number of represen-  
55 tation of fabrics the first kind of behavior represents fabrics with initial planes in horizontal direction.  
56 In this case a satisfactory approximate theory of membrane bending by lateral loads can be used  
57 with great realism and small complexity. If the initial plane of the textile to be represented is mainly  
58 vertical, it corresponds to the second kind above (almost all the applications for fashion design), and  
59 the approach will have to account for the buckling of the membrane. Buckling behavior in all struc-  
60 tures (bars, beams, membranes, plates or shells) is much more complex than bending [8]. This paper  
61 presents equations for simple and fast representation of the way in which a vertical cloth will fold  
62 (second kind of behavior) and compares the results obtained from these equations with real cloth  
63 behavior.

### 64 3 Tension field theory

65 The tension field theory describes the highly wrinkled state of membranes subjected to displacements  
66 well in excess of that necessary to initiate buckling. The assumption of zero flexural membrane stiffness  
67 on post-buckling and wrinkles at right angles to the lines of tension characterizes this theory. Mansfield  
68 [6] considers an initially flat membrane of arbitrary shape and variable stiffness, under self-weight  
69 supported in a vertical plane. Slack in the membrane manifests itself in the formation of wrinkle  
70 lines whose determination is the prime objective. The tension field theory was conceived as a theory  
71 of wrinkling isotropic elastic membranes, but the basic assumptions do not depend on isotropy or  
72 elasticity [7]. The membrane may have anisotropy related to the weave and nonlinear elastic properties  
73 [9]. Pipkin's derivation [7] takes into account that there is resistance to changes in the angle between  
74 the weft and warp directions in fabrics. However the theory does not attempt to describe the field  
75 of displacements normal to the membrane surface. Rimrott and Ma [10] use this theory to prevent  
76 wrinkles in substratum of solar panels. They [10] simulated, in laboratory, blankets with in-plane  
77 loading and their experiments showed that the number of wrinkles was a function of the critical  
78 stress that the material withstand. Theory and experiment are compared with good agreement [10].  
79 However, like the other works using tension field the description of the 3D wrinkled displacement is  
80 not considered. This displacement is much important for realistic visualization of textiles and related  
81 to the out-of-plane displacements engendered by the buckling action of the compressive stresses [9].  
82 Strictly speaking such relations are nonlinear and their exact analysis presents formidable difficulties  
83 [9]. Fortunately, textiles can easily be experimented in laboratory and their out-of-plane displacements  
84 can be measured to improve assumptions to derive the 3D equations [11].

#### 85 3.1 The wrinkle model from tension field assumptions

86 A distinctive property of textile materials is their extremely low compressive stiffness. A general  
87 assumption is that a textile cannot support any compressive stress. For the case when the vertical  
88 membrane is suspended by fixed points, the wrinkle lines have to pass through these fixed points  
89 in order to satisfy equilibrium conditions [6], whose solution will depend on the boundary condi-  
90 tion of each problem. From equilibrium conditions Mansfield [6] developed wrinkle lines equations for  
91 membranes (supported at points or edge-supported) with different boundary: cosine, parallelogram,  
92 triangular, pennant-shaped and wedge-shaped (see figure 1). Mansfield shows the wrinkle line equa-  
93 tions occur in a repetitive sequence in case of strip supported at intervals (figure 2). The case of  
94 inclined supports was also considered and demonstrated that the pattern of wrinkle lines is obtained  
95 from the previous case by a simple shearing process (as the parallelogram on figure 1 that is derived  
96 from rectangular shape).

97 The simplest wrinkle line solution [6] is given by

$$y = a_o e^k \cos(\pi x/l) \quad (1)$$

98 where  $a_o$  represents the maximum height of the first wrinkle (amplitude of cosine curve),  $l$  is the  
99 distance between fixed points or supports (figure 3), and

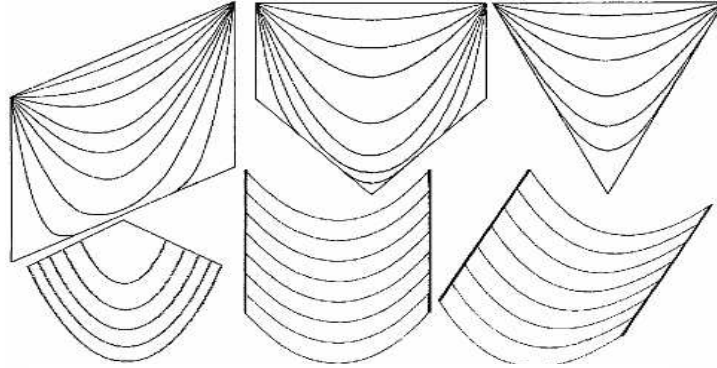


Figure 1: 2D wrinkle lines from tension field theory [6].

$$k = -(\pi^2 F)/(l^2 w) \quad (2)$$

100 where  $w$  is the textile weight per area (textile total weight,  $W$ , divided by the area of its surface) and  
 101  $F$  is the tension in the horizontal direction. This solution is exact for cosine-shaped textiles, that is  
 102 when the lower boundary (first wrinkle line) is given by

$$y_o = a_o \cos(\pi x/l)$$

103 and the upper boundary (upper wrinkle line) is given by

$$y_n = a_n \cos(\pi x/l) \quad (3)$$

104 In the limiting case we have  $a_n = 0$ , which corresponds to a straight upper boundary. Note that  $F$   
 105 is zero on  $y_o$ , which agrees with equilibrium requirement of free stress lower boundary. When  $a_n \rightarrow 0$   
 106 the horizontal component  $F$  grows to infinity.

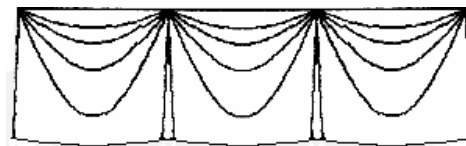


Figure 2: Repetitive folds in case of fabric strip supported at intervals.

107 Observing the behavior of actual suspended fabric it is possible to see that a finite number of  
 108 wrinkles will be developed [11]. The amplitude of the wrinkles is strongly dependent on the horizontal

109 motion of the supports but this is not the case for the number of wrinkles [12]. In experiments this  
 110 number are also not dependent of warp directions. We have investigated carefully this problem because  
 111 most of fabrics have anisotropy, but all results related with the wrinkles position and shape show not  
 112 direction dependence [13]. A more important observation is that there is not randomness in the fold  
 113 shapes [10–16]. In steady state, repetitions of experiments using the same initial conditions always  
 114 agree with this observation [11–16].

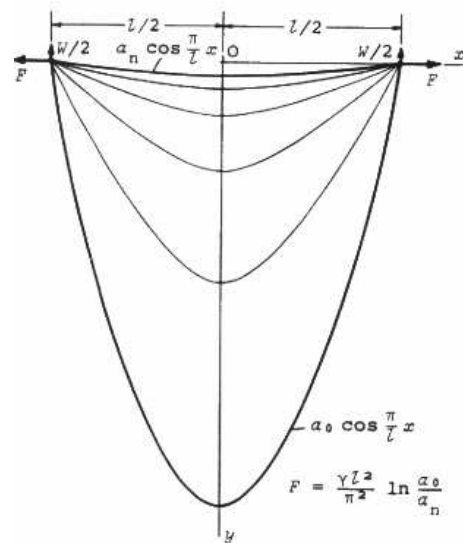


Figure 3: Cosine membrane and its wrinkle characteristics used in the equations.

115 **4 Simulating 3D wrinkles**

116 The tension field theory [9] considers only the 2D locus of the fabric folds (figure 1). Even if complicated  
 117 types of crinkle are considered, as those treated by Pipkin [7] of two intersected families of fold  
 118 lines or double folds, the wrinkle description is purely on plane. Of course the number of folds and  
 119 their locus is the main aspect of the cloth representation. However, folds must be 3D in realistic  
 120 textile visualization. Strictly speaking such problems are nonlinear and their exact analysis presents  
 121 formidable difficulties [9]. Fortunately, textiles can easily be experimented in laboratory and their  
 122 out-of-plane displacements can be studied to improve assumptions to derive the 3D equations [11].  
 123 To aid displacement descriptions, experiments have been organized with fabrics of different materials  
 124 and several shapes [13].

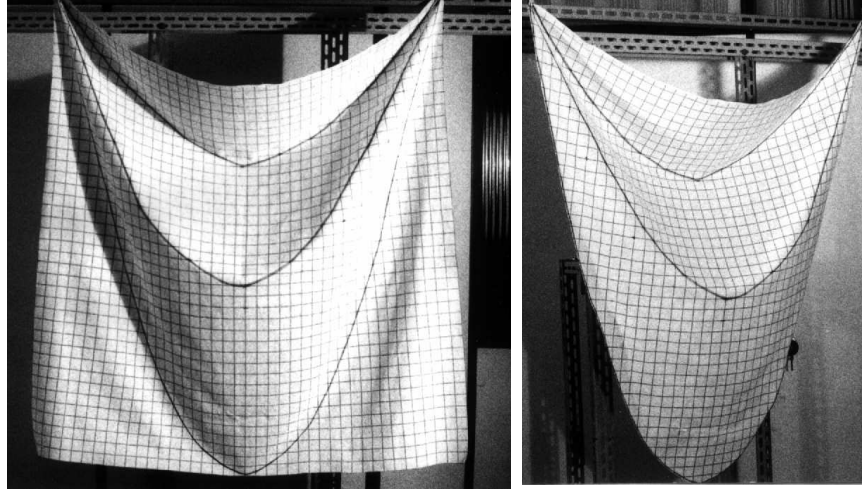


Figure 4: The same fold prevision from the proposed approaches are drawn on the real textiles. The match is inadequate only for the lowest wrinkle in non-cosine shapes. For these figures  $h = L = 140$  cm,  $t = 0.4$  mm. The material presents  $E = 40$  MPa,  $w = 17.7 \times 10^7$  N/mm<sup>2</sup>. The calculated values are  $n = 4$ ,  $Q=0.6$  and  $z_{max} = 7$  cm.

125 Experiences has been conducted comparing cosine with others types of boundaries and the results  
 126 showed that the wrinkle pattern is visually identical until the bottom wrinkle [12]. Quadrilateral  
 127 boundaries were the case with worse results. Figure 4 shows the drawings in real cloth of the wrinkled  
 128 prevision. The real cloths have rectangular boundary and cosine shapes. Both drawings are obtained  
 129 from considering the cosine expressions of the last section. The only position where the prevision and  
 130 the real folds visually do not match (see figure 4) is for the rectangular shape on the wrinkle whose  
 131 amplitude goes through the bottom boundary. But locus and shapes can be considered correctly  
 132 described for textile computer graphics representation. These experiences indicated that the use of  
 133 the 3D cosine boundary developed expressions is also adequate for other shapes [11]. The same happens  
 134 with the assumption of the lateral displacement. The displacement in  $z$  direction (normal to the  $xy$   
 135 plane of figure 3 or the lateral displacement) varies linearly on any strip folded between a + or -  
 136 direction, with maximum value for  $x = 0$ . The  $z$  component of the wrinkle line of order  $i$  can be  
 137 represented

$$z_i = z_{max} \cos(\pi x)/l \quad (4)$$

138 Then, the fabric representation can be performed in three steps: (1) grid generation; (2) determi-  
 139 nation of the elements related to the folds; and (3) the grid displacement and its combination with  
 140 other displacements (figure 5) and rendering techniques (but this is out of the scope of this work).

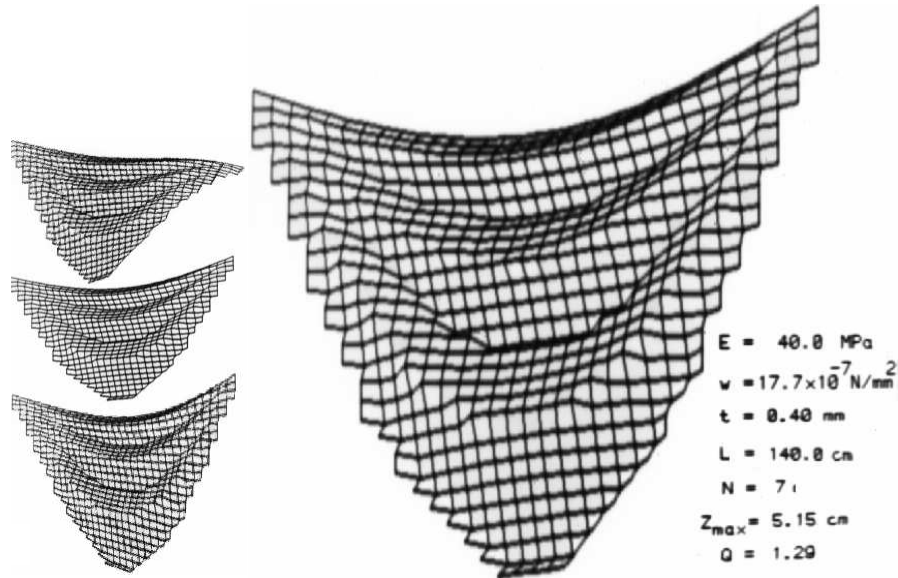


Figure 5: Results of the computer program implemented: The deformed grid for cosine membrane with the characteristics defined in the central line of Table 1, and examples of addition with other deformations and displacements.

#### 141 4.1 First step: grid generation

142 This step represents the cloth modeled as a grid of three-dimensional coordinates. By increasing the  
 143 density of the grid, greater resolution of the surface model may be obtained. A distinction must be  
 144 made between free points and restricted points on the grid. The restricted points are those that fix a  
 145 piece of fabric, their coordinates will not change. The remaining points are considered as free points,  
 146 they will move with textile folds and their new position must be computed. The grid is treated as a  
 147 coordinate system that describes the garment shape before the appearance of folds. Each grid point  
 148 should be corresponded with a fabric point on  $x, y$  and  $z$  axes.

#### 149 4.2 Second step: determination of fold positions

150 To determine the displacement of each point when the textile is suspended and the folds appear,  
 151 the locus of the wrinkles must be computed. For this some parameters must be calculated. They are  
 152 the number of wrinkles,  $n$ , the amplitude of each wrinkle in vertical direction,  $a_i$ , and the maximum  
 153 component of the wrinkle lines out of the initial plane,  $z_{max}$ . The placement of each point of the grid  
 154 on the folded fabric, which will be determined in the next step, is related to these values.

155 The process of determining these parameters involves an iterative stage. It has been shown [10] for

156 cosine boundaries (figure 3) that the wrinkle amplitudes grow in geometric progression. Hence, for  
 157 each wrinkle  $i$ , the parameter  $a_i$  in equation (3) can be described as

$$a_0/a_1 = a_1/a_2 = \dots = a_{n-1}/a_n = (a_0/a_n)^{1/n} = Q \quad (5)$$

158 So the vertical position of each fold is:

$$y_i = (a_0/Q^i) \cos(\pi x/l) \quad (6)$$

159 However, the value of the ratio  $Q$ , and the number of wrinkles  $n$  are not yet determined. Since  
 160 the critical stress,  $\sigma_{cr}$ , cannot be exceeded, the number of wrinkles and their amplitudes will adjust  
 161 themselves. This stress is limited by the buckling stress [8]. The ratio  $Q$  can be related to the maximum  
 162 compressive stress in the cloth [11]:

$$wh(Q-1)^2/(tQ(Q+1)) \leq \sigma_{cr} = cEt^2/(l^2(1-\nu^2)) \quad (7)$$

163 where  $t$  is thickness of the cloth,  $h$  is its height or its initial maximum on the vertical dimension,  $c$  is  
 164 a constant describing the load condition [8],  $E$  is the material Young's modulus and  $\nu$  its Poisson's  
 165 ratio.

166 As a first approach  $Q$  can be obtained from (7) by enforcing equality and using the maximum  
 167 compression stress of thin plates [6]. The other two unknowns  $n$  and  $z_{max}$  are obtained by fabric  
 168 inextensibility assumptions [11]. The initial length  $L$  and the wrinkled upper boundary length can be  
 169 related by

$$L = \int_{-l/2}^{l/2} \sqrt{1 + \left(\frac{dy_n}{dx}\right)^2 + \left(\frac{dz_n}{dx}\right)^2} dx$$

170 or from (4) to (6)

$$L = \int_{-l/2}^{l/2} \sqrt{1 + \left(\frac{\pi}{l}\right)^2 \left(\frac{a_0^2}{Q^{2n}} + z_{max}^2\right) \sin^2 \frac{\pi x}{l}} dx \quad (8)$$

171 The inextensibility of the vertical fibers leads, for  $x = 0$ , to

$$h = \sum_{i=1}^n \sqrt{(a_{i-1} - a_i)^2 + (2z_{max})^2}$$

172 or from (5) and (6)

$$h = \sum_{i=1}^n \sqrt{\frac{a_0^2}{Q^{2(i-1)}} \left(1 - \frac{1}{Q}\right)^2 + (2z_{max})^2} \quad (9)$$

173 An approximation of  $n$  can be determined by means of the equation (5):

$$n = \text{Int} [\log (a_0/a_n) / \log Q] \quad (10)$$

174 in which  $\text{Int} [.]$  is the integer approximation  $[.]$ , because the number of wrinkles must be integer.  
 175 However,  $a_0$  and  $a_n$  are both unknown. They are the amplitudes of the lower and upper boundaries  
 176 of the folded fabric (figure 3). As a first approximation  $a_0 = 1.01h$  and  $a_n = 0.01h$  can be used (for  
 177 practical purposes) beginning the iterative approach. The obvious  $a_n = 0$  is out of the question in  
 178 equation (10) (indetermination). These values are used as an initial approximation. As soon as  $n$  and  
 179  $Q$  become know, the amplitude  $a_i$  of each wrinkle line can be obtained from (5). A tentative value  
 180 must be used for  $z_{max}$  (as  $0.01h$ ) in the equation (8) and (9).

181 In this work a numerical integration (Simpson) is used to solve equation (8). Note that its result is  
 182 a first approximation of horizontal textile length,  $L'$ , where the real value  $L$  is known. The obtained  
 183 value of  $L'$  is tested against the real value and new values of  $z_{max}$ , and  $n$  are obtained using above  
 184 equations, until the convergence of  $L'$  to  $L$ . The tolerance value of this convergence is more or less  
 185 arbitrary, depending on the desired accuracy. In every case on the next section 5% is used as tolerance  
 186 value.

### 187 4.3 Third step: wrinkle line positions and grid displacement

188 The third step performs a 3D displacement on all points on the surface. After determining of the basic  
 189 parameters  $Q$ ,  $z_{max}$  and  $n$ , the wrinkles lines and all locations of fold points can be obtained by using  
 190 equations (3), (4) and (5). Knowing the position of the folds, the 3D visualization of the deformed grid  
 191 is straightforward from interpolation between consecutive folds and the surface is ready for projections,  
 192 shadings, shadows and textures details. Figure 5 shows on the main illustration the deformed grid and  
 193 in the small illustrations the results of the deformed grid added to other displacements or deformations  
 194 (as in animation sequences).

## 195 5 Results and conclusions

196 Only the elements related to the wrinkle locus are here presented. First, numerical results consider the  
 197 length influence on wrinkles. To study this the same textile with increasing length,  $h$ , in one direction  
 198 is used in simulations. The other characteristics were kept and they are  $t = 0.25$  mm,  $E = 165$  MPa,  $w$   
 199  $= 15 \times 10^{-7}$  N/mm<sup>2</sup> and  $L = 140$  cm. The support displacement is 10 cm, so  $l = 120$  (figure 3). Table  
 200 1 shows the parameters obtained by the approach for each  $h$ . The number of wrinkles increases when  
 201 the length increases. For rectangular shapes, these results can easily be compared with laboratory  
 202 experiments. Figure 5 shows the wrinkle line positions and grid displacement obtained for this fabric  
 203 with cosine shape and  $h = 140$  cm.

204 Obtained fold characteristics for textiles with  $145 \times 90$  cm and increasing weight are shown in Table  
 205 2. The other characteristics are  $t = 0.35$  mm,  $E = 150$  MPa and support displacements of 8.5 cm.  
 206 These results show that the number of wrinkles increases with the weight. A series of simulations  
 207 have been done for textiles with  $90 \times 75$  cm and increasing thickness,  $t$ , as shown in Table 3. The  
 208 other characteristics for the results (of Table 3) are  $w = 12.8 \times 10^{-7}$  N/mm<sup>2</sup>,  $E = 185$  MPa, and

209 support displacement of 7 cm. The effect of increasing stiffness is clearly seen. Some results obtained  
 210 for textiles with length of  $125 \times 85$  cm and increasing Young's modulus,  $E$ , are shown in Table 4. The  
 211 other characteristics are  $t = 0.23$  mm,  $w = 17 \times 10^{-7}$  N/mm<sup>2</sup> and support displacement of 9 cm. It  
 212 shows that, when the elasticity increases, the ratio  $Q$  increases, but the number of wrinkle decreases.

Table 1: Results for a increasing length.

$h$ (cm)	$n$	$z_{max}$ (cm)	$Q$
90	5	5.4	1.31
140	7	4.8	1.29
235	8	6.0	1.34

Table 2: Fabric with increasing weight.

$w$ ( $10^{-7}$ N/mm <sup>2</sup> )	$n$	$z_{max}$ (cm)	$Q$
10	4	5.60	1.78
33	6	4.60	1.46
54	7	4.40	1.39

Table 3: Fabric with increasing thickness.

$t$ (mm)	$n$	$z_{max}$ (cm)	$Q$
0.09	7	3.45	1.33
0.26	4	4.15	1.65
0.40	2	1.10	2.60

Table 4: Fabric with increasing elasticity.

$E$ (MPa)	$n$	$z_{max}$ (cm)	$Q$
55	8	3.70	1.34
110	7	4.25	1.30
185	6	4.55	1.47

213 Beside numbers, side by side comparison of real cloth and simulation of the same cloth is a better  
 214 argument for the visual similarity obtained with the approach. Figures 6 and 7 show the locus of the  
 215 folds drawn over real cloths. The wrinkle lines behavior is considered in cosine formulation for both  
 216 cases (according to the experimental investigations).

217 Results of this approach show that it is possible to represent the fold peculiarities related with textile  
 218 geometry and physical characteristics. The introduced out-of-plane analysis of the displacements allows  
 219 to represent the post-wrinkling state. The derived equations provide the basic variables for realistic  
 220 appearance of clothes: number of wrinkles and their position. The resulting deformed description can  
 221 be used then with a variety of rendering for realistic textile representation [1, 2].

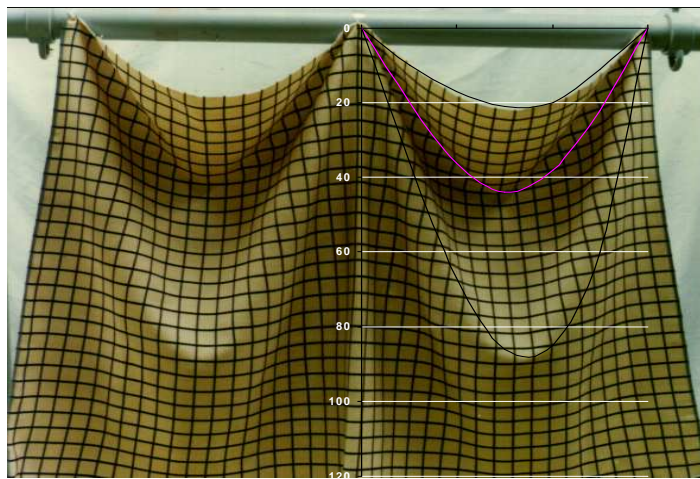


Figure 6: Folds obtained by the approach drawn over a real cloth supported at intervals (red lines represent negative folds).



Figure 7: Folds obtained by the approach drawn over a real shirt (red lines represent negative folds).

## 222 References

- 223 [1] Dai, M.L. & Ozawa, K., Simulation of worn-out cloth textures by doubly stochastic l-systems.  
 224 *Image and Vision Computing*, **16**, pp. 363–371, 1998.
- 225 [2] Gray, S., In virtual fashion. *IEEE Spectrum*, **35(2)**, pp. 18–25, 1998.
- 226 [3] Ng, H. & Grimsdale, R., Computer graphics techniques for modeling cloth. *IEEE Computer  
 227 Graphics and Applications*, **16(5)**, pp. 28–41, 1996.
- 228 [4] Eischen, J., Deng, S. & Clapp, T., Finite-element modeling and control of flexible fabrics parts.  
 229 *IEEE Computer Graphics and Applications*, **16(5)**, pp. 71–80, 1996.
- 230 [5] Chen, B. & Govindaraj, M., A physically based model of fabric drape using flexible shell theory.  
 231 *Textile Research Journal*, **65(6)**, pp. 324–330, 1995.
- 232 [6] Mansfield, E., *Gravity-induced wrinkle lines in vertical membranes*, volume A 375. Royal Society:  
 233 London, 1981.
- 234 [7] Pipkin, A., Continuously distributed wrinkles in fabrics. *Arch Rational Mech Anal*, **95**, pp. 93–115,  
 235 1986.
- 236 [8] Brush, D. & Almroth, B., *Buckling of Bars, Plates and Shells*. McGraw-Hill: New York, 1975.
- 237 [9] Mansfield, E., *Analysis of wrinkled membranes with anisotropy and nonlinear elastic properties*,  
 238 volume A 353. Royal Society, 1977.
- 239 [10] Rimrott, F. & Ma, X., Tension field theory and spacecraft solar panels. *8th Symposium on Engi-  
 240 neering Applications of Mechanics*, Sherbrooke, 1986.
- 241 [11] Segenreich, S. & Conci, A., Displacement behavior of a vertically suspended piece of cloth. *CSME  
 242 Mechanical Eng. Forum*, Toronto, volume 2, 1990.

- 243 [12] Rimrott, F. & Cvercko, M., Wrinkling in thin plates due to in-plane body forces. *IUTAM Symp. on*  
244 *Inelastic Behavior of Plates and Shells*, Rio de Janeiro, 1985.
- 245 [13] Conci, A. & Segenreich, S., On the number of wrinkles in a rectangular membrane. *II Pan*  
246 *American Congress of Applied Mechanics*, Vina del Mar, 1991.
- 247 [14] Libai, A. & Givoli, D., Analysis of pulled axisymmetric membranes with wrinkling. *International*  
248 *Journal of Solids and Structures*, **39(5)**, pp. 1259–1274, 2002.
- 249 [15] Coman, C., On the applicability of tension field theory to a wrinkling instability. *Acta Mechanica*,  
250 2006.
- 251 [16] Coman, C. & Haughton, D., Localized wrinkling instabilities in radially stretched annular thin  
252 films. *Acta Mechanica*, **185(3-4)**, pp. 179–200, 2006.